

General Disclaimer

One or more of the Following Statements may affect this Document

- This document has been reproduced from the best copy furnished by the organizational source. It is being released in the interest of making available as much information as possible.
- This document may contain data, which exceeds the sheet parameters. It was furnished in this condition by the organizational source and is the best copy available.
- This document may contain tone-on-tone or color graphs, charts and/or pictures, which have been reproduced in black and white.
- This document is paginated as submitted by the original source.
- Portions of this document are not fully legible due to the historical nature of some of the material. However, it is the best reproduction available from the original submission.

Transient Technique for Measuring Heat Transfer Coefficients on Stator Airfoils in a Jet Engine Environment

(NASA-TM-87005) TRANSIENT TECHNIQUE FOR
MEASURING HEAT TRANSFER COEFFICIENTS ON
STATOR AIRFOILS IN A JET ENGINE ENVIRONMENT
(NASA) 17 p HC A02/MF A01 CSCI 14B

N85-25794

63/35 Unclass
21134

Herbert J. Gladden and Margaret P. Proctor
Lewis Research Center
Cleveland, Ohio

Prepared for the
Twenty-first Joint Propulsion Conference
cosponsored by the AIAA, SAE and ASME
Monterey, California, July 8-10, 1985

NASA



TRANSIENT TECHNIQUE FOR MEASURING HEAT TRANSFER COEFFICIENTS
ON STATOR AIRFOILS IN A JET ENGINE ENVIRONMENT

Herbert J. Gladden and Margaret P. Proctor
National Aeronautics and Space Administration
Lewis Research Center
Cleveland, Ohio 44135

Abstract

A transient technique was used herein to measure heat transfer coefficients on stator airfoils in a high-temperature annular cascade at "real engine" conditions. The transient response of thin film thermocouples on the airfoil surface to step changes in the gas stream temperature was used to determine these coefficients. In addition, gardon gages and paired thermocouples were also utilized to measure heat flux on the airfoil pressure surface at steady state conditions. The tests were conducted at exit gas stream Reynolds numbers of one-half to 1.9 million based on true chord. The results from the transient technique show good comparison with the steady-state results in both trend and magnitude. In addition, comparison is made with the STANS boundary layer code and shows good comparison with the trends. However, the magnitude of the experimental data is consistently higher than the analysis.

Nomenclature

A	amplitude ratio of the Fourier components of the wall to gas temperatures
C_p	specific heat of wall material, J/kg·K
DTM	differential temperature, μv
f	frequency of Fourier component, Hz
$h_{g,ss}$	heat transfer coefficient measured with steady-state instrumentation, $\text{W/m}^2\cdot\text{K}$
$h_{g,T}$	heat transfer coefficient measured with transient technique, $\text{W/m}^2\cdot\text{K}$
k	thermal conductivity of wall material, $\text{W/m}\cdot\text{K}$
λ	distance into airfoil well, m
q	heat flux measured by steady-state heat flux gages, W/m^2
t	time, sec
$T(\lambda, f)$	amplitude of the Fourier component at λ , K
T_g	gas temperature, K
$T_g(f)$	amplitude of the gas temperature Fourier component, K
T_w	wall temperature, K
$T_w(f)$	amplitude of wall temperature Fourier component, K

x/L	normalized distance along vane surface from leading edge, dimensionless
α	thermal diffusivity of wall material, m^2/sec
ρ	density of wall material, kg/m^3

Introduction

Improved performance of turbojet and turbofan engines is typically accompanied by increased cycle pressure ratio and combustor exit gas temperature. Gas pressure levels of 25 to 30 atm and gas temperatures of 1600 K exist in some current operational engines while pressure levels up to 40 atm with gas temperatures of 1800 K are anticipated in advanced commercial engines. These continuing increases in the turbine entry gas pressure and temperature of the modern gas turbine engine and the high development cost puts a premium on an accurate initial aerothermal design of the turbine hot section hardware.

The design goals for commercial jet engines include high cycle efficiency, increased durability of the hot section components (lower maintenance costs), and lower operating costs. These goals are contradictory in that high cycle efficiency requires minimizing the cooling air requirements while increased durability requires metal temperatures and temperature gradients to be minimized. An optimum design can only be realized through an improved understanding of the flow field and the heat transfer process in the turbine gas path.

Sophisticated computer design codes are being developed which have the potential of providing the designer with significantly better initial estimates of the flow field and heat load on the hot section components. These codes are being evaluated and verified through low temperature and pressure research in cascades and tunnels. However, by design, these facilities do not model all of the processes that exist in a real engine environment, and therefore, the ability of the design codes to predict the interaction of the various parameters cannot be fully evaluated.

The Hot Section Facility at the NASA Lewis Research Center provides a "real-engine" environment with established boundary conditions and convenient access for advanced instrumentation to study the aerothermal performance of turbine hot section components. The thermal performance and, ultimately, the life of these components in a realistic application is dependent on the designer's ability to predict the local heat load distribution. The stator airfoil heat transfer coefficient distribution presents a particularly challenging situation for the designer because of the complex

flow field through the turbine. Even though heat transfer on airfoils has been studied for several years, there is a limited amount of realistic data available to verify the analytical models. Measurement of heat flux in both a test rig and an engine environment is desirable as a means of verifying or improving the designers prediction capability.

Several techniques have been used to measure heat flux to (from) turbine stator vane airfoils. These measurements have been made primarily in test rigs at simulated engine conditions. Both steady state tests (using gardon gages, paired thermocouples, heater strips, and calorimetry) and transient tests (using blow-down tunnels and shock tubes) have been utilized. In addition, Dils¹ has suggested a transient technique using the fluctuating gas temperature as the driver.

This report uses an adaptation of the Dils method and that of Berry² and Beacock³ to determine the heat transfer coefficients on stator airfoils operating at "real engine" conditions. The dynamic response of thin film thermocouples to the random pulses of the gas temperature were analyzed and used to determine the local heat transfer coefficients. In addition, gardon gages and paired thermocouples were used to measure heat flux on the stator pressure surface.

The tests were conducted in the HSF cascade rig at gas stream temperatures and pressures up to 1400 K and 13 atm. These conditions correspond to exit gas stream Reynolds numbers up to 1.9 million based on true chord.

The data are presented as a heat transfer coefficient distribution around the stator airfoil. In addition, comparisons are made with the gardon gages and paired thermocouples as well as analytical results from the STAN5 boundary layer code.

Facility

General Description

The Hot Section Facility (HSF) is shown in a perspective view in Fig. 1(a). The HSF is a unique facility having fully-automated control of the research rig through an integrated system of mini-computers and programmable controllers. The major components of this facility and how they interface to provide a real engine environment are discussed in more detail in Refs. 4 and 5.

Combustion air is provided to the facility at 10 atm through a nonvitiated preheater which modulates the air temperature between ambient and 560 K. A 20-atm mode of operation can be selected which provides combustion air at pressures up to 20 atm and temperatures up to 730 K when utilizing the heat of compression of a 2:1 compressor.

Digital Control Center

The operation and data acquisition for the facility are fully automated through an integrated digital minicomputer system called the Digital Control Center (DCC).^{4,5} Four interconnected mini computers make up the DCC. Each computer has a dedicated task and is identified according to its primary task (eg., Input, Control, Operation, and

Research computers). The Control computer was the key link to the successful completion of the research described herein.

The Control computer's task is to control 19 highly interactive process variables at update rates of 20 to 150 times/sec. All test conditions are stored in the Operations computer prior to a test run and are passed to the Control computer when the operator requests a change in conditions. In addition, the operator can request a step change in a process variable through the Setpoint Entry Keyboard. This feature was used to create step changes in the combustor exit temperature at known frequencies to drive the transient conduction process.

Cascade Configuration

A cross-sectional schematic of the HSF cascade is shown in Fig. 1(b). The major components consist of a heat source (combustor), the full annular vane row, an exhaust duct, a quench system (to lower temperature of the exhaust gas), and the exhaust system.

The vane row consists of 36 stator vanes. The 36 vanes are separated into two groups: 10 test vanes and 26 slave vanes. The test vane and slave vane cooling air is supplied from two separate manifolds with the flow rates to each manifold independently computer controlled. The primary instrumentation for these tests were in the slave vane sector.

Stator Vane

The stator vane configuration used for these tests was a hollow shell without an insert to augment the coolant-side heat transfer. The cooling air was supplied to the vane through the vane tip and exhausted into a plenum at the vane hub. Because the leading and trailing edge regions were undercooled, the combustor exit gas temperature was restricted to maintain reasonable metal temperatures in the airfoil.

The vane row hub and tip diameters were 0.432 and 0.508 m, respectively. Both the vane height and chord were 3.81 cm. More detailed geometric data are given in Table 1 and Ref. 5.

Instrumentation

The primary instrumentation used for these tests were a dual-element, fast response gas temperature probe and thin film thermocouples to measure the airfoil surface temperature. Other conventional steady state instrumentation such as gas total temperature and pressure probes and airfoil surface temperature and pressure sensors were used to monitor the test conditions. Gardon-type and paired thermocouple heat flux gages were also installed on selected airfoil pressure surfaces.

The dual-element gas temperature probe was located at the combustor exit, 263° ccw from top dead center locking downstream. The probe sensors are shown in Fig. 2. The two thermal elements of the probe were platinum 30 percent rhodium/platinum 6 percent rhodium (type B) and were 0.076 and 0.25 mm in diameter, respectively. The probe construction is described in more detail in Ref. 6.

The airfoil surface temperature response was measured by thin film thermocouples sputtered on the gas-side surface of four vanes. These vanes were located circumferentially at 90° ccw $+30^\circ$. The thermal elements were platinum/platinum 10 percent rhodium (type S). Each thermal element of the thermocouple was 1.27 mm wide by 12 μ m thick forming a junction of ~ 1.27 mm in the chordwise direction. A 2.5 to 3.0 μ m thick substrate of Al_2O_3 served as an insulator between the thin film and the airfoil wall. A typical application of the thin film thermocouples is shown in Fig. 3. Typically, there were four thermocouples on one surface of the airfoil and two thermocouples on the opposite surface. The distribution of thin film thermocouples is given in Table 2.

Two types of heat flux gages were installed on the pressure surface of four airfoils. There were four gardon-type gages on two airfoils and four paired thermocouple-type gages on each of two airfoils. These airfoils were located circumferentially at 270° ccw $+15^\circ$. These gages were installed and calibrated by Pratt and Whitney Aircraft following the procedure outlined in Ref. 7. The location of these gages are given in Table 2. When heat flux gage data were recorded, the dual-element probe was replaced with a conventional aspirated total temperature probe.

Research Data System

The research computer controls the steady state data gathering process on command. During the data taking cycle, the research computer prepositions the radially traversed probes, records and stores raw data, increments the probes to a new position and repeats the process until the cycle is complete. The raw data is then converted to engineering units, packaged, tagged with a unique number, and transferred to the Central Data Collector for further processing and storage.

The purpose of these tests was to determine heat transfer coefficients through the transient response of the airfoil wall temperatures to changes in the gas temperature. To accomplish this, it was necessary to simultaneously record the time history of both the dual-element gas temperature probe and the thin film thermocouples as the gas temperature was stepped at several frequencies. Both the dc and ac outputs of these instruments were recorded simultaneously on FM tape. Low noise ac and dc amplifiers with gains of 100 to 1000 were used to obtain signals with sufficient magnitude to be recorded on the FM tape. Because of FM tape channel limitations only four thin film thermocouples could be recorded simultaneously for a given series of runs.

Experimental Procedure

The gas conditions were established by setting the combustor inlet total pressure, the vane exit outer-radius static pressure, and the combustor fuel/air ratio to predetermined input values stored in the Operations computer. The coolant flow rate and temperature were also fixed at predetermined input values.

The Setpoint Entry Keyboard was then used to step the combustor exit temperature between the input value and a 140 K increment at a given

frequency. The test conditions are summarized in Table 3.

Analytical Procedure

Model

The transient heat transfer model of Dils¹ was used to determine the heat transfer coefficients on the airfoils tested. However, where Dils used the inherent gas temperature fluctuation from the combustion process, the data obtained herein were the result of imposed step changes in the gas temperature at known frequencies.

In a semi-infinite solid subject to periodic temperature boundary conditions, the Fourier components of the surface temperature are attenuated according to the relation:

$$T(x, f) = T_w(f) \exp\left(-\frac{\pi f}{\alpha} x\right) \cos\left(\sqrt{\frac{\pi f}{\alpha}} x - 2\pi f t\right) \quad (1)$$

If the thermal wavelength, $\sqrt{\alpha/\pi f}$, is small with regard to the dimensions of the body and the local heat transfer coefficient on the surface is constant within the bandwidth of the surface temperature wave, then the amplitudes of the Fourier components of the surface temperature and the gas temperature are related by the approximation:

$$\frac{T_w(f)}{T_g(f)} = \frac{h_g T}{\sqrt{2\pi f \rho C_p k}} \quad (2)$$

There is a 45° phase lag between the Fourier components of the surface and gas temperature waves. If the thermal properties of the airfoil wall are known and the amplitude ratio of the Fourier components can be determined, then the local heat transfer coefficient can also be determined.¹

Data Reduction

Dynamic measurements of the gas and wall temperatures were recorded on FM tape while the gas temperature was ramped between high and low temperatures at several frequencies. The FM tape was then digitized at a sampling rate twice the highest frequency of interest or 25 samples/sec. The dc channels of each digitized reading were stripped out to identify the exact length and location of each ramping event. This information was entered in an input file. An IBM 370 was used to read the input file and the digitized data and to take the transfer function between the gas temperature and the wall temperature (i.e., the dc dual element channel and the dc thin film channel). The amplitude ratio, $A = T_w(f)/T_g(f)$, was then plotted against frequency for those frequencies where the phase angle was $-45 \pm 5^\circ$ and the coherence was >0.8 . A line with a slope of $-1/2$ was then drawn through the data as Dils' theory requires and the heat transfer coefficient was calculated from Eq. (2).

Analysis

The STAN5^{8,9} boundary layer code was used to calculate the expected heat transfer coefficient distribution around the stator airfoil. Since all tests were made at the same nominal gas temperature conditions the primary variable was the gas pressure which was used to establish the Reynolds number. The stator inlet and exit critical velocity

ratios were also kept constant at design values. The design critical velocity ratio distribution around the airfoil is shown in Fig. 4. Experimental measurements also shown in Fig. 4 agree well and justify the use of this velocity ratio distribution in the STAN5 boundary layer code. The stator inlet turbulence level was assumed to be 10 percent.

The boundary layer on the pressure surface was forced to a turbulent solution at a point forward of that predicted by the transition models in STAN5. The start and finish of transition was assumed to be at an x/L of 0.044 and 0.10, respectively. The boundary layer transition point on the suction surface was determined by the Van Driest and Blumer model while the length of transition was determined by the Abu-Ghanman and Shaw model.

Heat Flux Gage

The heat flux at selected locations on the airfoil pressure surface was determined by the measurement of wall temperature and a temperature differential and converting these measurements to heat flux through a sensor calibration.

$$q = \frac{DTM}{\text{sensitivity}} \quad (3)$$

where the sensitivity is determined from calibration and has units of $\mu\text{V}/\text{W}/\text{m}^2$. Local heat transfer coefficients were then calculated using the gas temperature measured at the combustor exit mean radius and the local wall temperature.

$$h_{g,ss} = q/(T_g - T_w) \quad (4)$$

The gas temperature was measured in the sector where the heat flux gages were located.

Uncertainty Analysis

An uncertainty analysis¹⁰ was made with the goal of determining the uncertainty in the measured heat transfer coefficient. The heat transfer coefficient, $h_{g,T}$, is a function of the properties of the wall material, Mar M-509, frequency and the amplitude ratio, A . The sources of error used to determine the uncertainty of the gas temperature at 1255 K and the wall temperature at 810 K are shown in Table 4. The uncertainty of the frequency at 1 Hz was assumed to be ± 0.01 Hz and the uncertainty of density was assumed to be ± 0.1 percent. The uncertainty of the thermal conductivity was derived from the root mean square of a ± 4 percent uncertainty due to the aluminum oxide insulator between the airfoil wall and the thin film, a ± 4 percent uncertainty in the reported value¹¹, and a ± 0.8 percent uncertainty due to the wall temperature (± 1.6 percent). The uncertainty in specific heat was the root mean square of a ± 3.0 percent uncertainty in the reported value¹¹ and a ± 0.4 percent uncertainty due to the wall temperature. A ± 15 percent uncertainty based on the data scatter was used for the amplitude ratio. This resulted in a total uncertainty of ± 15.3 percent in the transient measured heat transfer coefficient. The uncertainty in the steady state measured heat transfer coefficient was calculated based on a ± 12 percent uncertainty in the heat flux measurement, a ± 60 K uncertainty in the gas temperature measurement, and a ± 1.0 percent uncertainty in the

wall temperature measurement. This resulted in a total uncertainty of ± 18 percent in the steady state measured heat transfer coefficient.

The spatial location of the thin film thermocouples is given in Table 2. The uncertainty in the location is 1.25 mm which is within ± 10 percent of the x/L locations given.

Results

The purpose of this paper is to present experimentally measured heat transfer coefficients obtained in a "real engine" environment by a transient technique, compare the results with steady state data and predicted heat transfer coefficients, and discuss the significance of the results.

Thin Film Thermocouples

Heat transfer coefficients were determined by repeatedly ramping the gas temperature between a low and a high temperature at several different frequencies and recording the transient response of the wall temperature. A portion of typical wall and gas temperature time histories shown in Fig. 5(a,b) illustrates the magnitude and shape of the transient input and the time response of the thin film thermocouple. Typically, the gas temperature was varied 140 K and the wall temperature responded with a variation of ~ 30 K. In Fig. 5, six repetitions of a 2 sec ramp cycle are followed by seven repetitions of a 4 sec ramp cycle. These and other ramp cycle lengths were used to gather data at fundamental frequencies from 0.005 to 0.5 Hz (periods of 200 to 2 sec).

The amplitude ratio of the Fourier components of the wall to gas temperatures was plotted against frequency on log-log paper. Data at $x/L = 0.262$ are shown in Fig. 6(a,b,c) for gas Reynolds numbers of 0.55×10^6 , 1.20×10^6 and 1.90×10^6 , respectively. Data at fundamental frequencies less than 0.05 Hz were deleted because the phase lag was less than 45° , thus violating a requirement in Dils' approximation. The data in Fig. 6 follow a slope of $-1/2$ and has a phase lag of about 45° as Dils' theory requires, justifying the use of that approximation to determine local heat transfer coefficients. The coherence function between the gas temperature ramp and the wall temperature response was greater than 0.8 which indicates that there was a significant relationship. The trend of increased heat transfer with increased Reynolds number is also indicated by the data.

Heat Transfer Coefficients

The experimental heat transfer coefficients on the airfoil pressure surface are shown in Fig. 7. The data are plotted as a function of the dimensionless surface distance, x/L . Also included on the figure is an analytical solution from the STAN5 boundary layer code.

Pressure surface. The low Reynolds number data (0.55×10^6) are shown in Fig. 7(a). The data from the transient experiment show generally laminar characteristics in the midchord region with a transition to turbulent flow near the trailing edge. The steady state experimental data from the gardon-gages and the paired thermocouples also show generally laminar characteristics in the midchord region with a magnitude of ~ 75 percent of the transient

data. The experimental data are also compared with an analytical solution that has been forced to a turbulent flow solution near the airfoil leading edge. This solution compares favorably with the steady state heat transfer coefficients but it is ~75 percent of the transient data.

The 1.2×10^6 Reynolds number data are shown in Fig. 7(b). The transient experimental data from the thin film thermocouples in the midchord and trailing edge region follow a trend suggesting boundary layer transition. However, the heat transfer coefficient, from the transient technique, in the leading edge region have relatively large magnitudes consistent with an augmented laminar boundary layer. The two transient measurements at x/L of 0.354 are from different vanes and show a significant difference in magnitude. Data up to an x/L of 0.354 are in an apparent transitional region indicated by the steep gradient in the heat transfer coefficient. The steady-state experimental data from the gardon-type and paired-thermocouple gages generally compares with the transient experimental data. The STAN5 analysis was also forced to a turbulent flow solution near the leading edge for this Reynolds number. The results in Fig. 7(b) show a good comparison between the analysis and the experimental data in both magnitude and trend.

Data for a Reynolds number of 1.9×10^6 are shown in Fig. 7(c). The heat transfer coefficients from both the transient and the steady-state measurements show the same trend in the midchord region. However, the steady-state data have a larger magnitude than the transient data at this Reynolds number, which is opposite of the relation shown in Figs. 7(a) and (b). The analytical solution shows a good comparison with the experimental heat transfer coefficients when the boundary layer is forced to a turbulent flow solution near the leading edge.

Suction surface. Experimental heat transfer coefficients from the transient technique are shown in Fig. 8 for the airfoil suction surface. The analytical solution from STAN5 follows the data reasonably well for all three Reynolds numbers. However, at an x/L of 0.62, the experimental heat transfer coefficient shows a substantial increase over the trend established by the other data. A sudden increase in heat transfer on a suction surface trailing edge is not uncommon and may be due to secondary flow effects. In addition, the analytical solution generally underpredicts the experimental results. And the magnitude of the underprediction increases with decreasing Reynolds number.

Discussion

The transient and steady state experimental data on both the airfoil pressure surface and the transient data on the suction surface show increasing magnitude with Reynolds number as would be expected. In addition, the experimental data trends are similar to those predicted by the STAN5 boundary layer code. Data from both transient and steady-state techniques on the pressure surface have similar magnitudes and trends. There is, however, a significant deviation in magnitude between the experimental heat transfer coefficients and those predicted by STAN5 in the laminar and transitional regions.

The strengths of the transient technique are its relative ease of installation on the airfoil surface without the precise fabrication steps required for the gardon-gages and the paired thermocouples. This also permits a greater density of thin film thermocouples to be installed on a given airfoil without affecting its structural integrity. In addition, the transient technique can measure the total convective heat transfer coefficient at the airfoil surface without the one-dimensional limitations of the steady-state gages.

However, the heat transfer experiment using a transient technique must be carefully planned to comply with the semi-infinite wall and constant coefficient assumptions of the experimental model. The assumption regarding small thermal wavelengths follows from the semi-infinite solid model. The thermal wavelengths for this study range from 5.32 mm to 1.68 mm for the frequencies 0.05 to 0.5 Hz, respectively. These are of the same order as the airfoil wall thickness of 1.3 mm because of the low frequency range. However, the low frequency range used satisfies the assumption that the local heat transfer coefficient on the surface is constant within the bandwidth of the surface temperature wave. The only change in heat transfer coefficient, while ramping the gas temperature, would be due to changes in fluid properties which are minor for a 140 K gas temperature increment. Also, the different circumferential orientation of the gas and wall temperature measurements may have contributed to the uncertainty of the heat transfer coefficients from the transient technique.

Concluding Remarks

The results of measuring heat transfer coefficients on turbine vane airfoils through a transient technique are presented and compared with steady state measurements and analysis. The results show good comparison with the steady state data. In addition, the experimental data trends are predicted by the STAN5 boundary layer code. However, the magnitude of the experimental measurements were not predicted by the analysis particularly in laminar and transitional regions near the leading edge.

Inability of the STAN5 boundary layer code to predict the heat transfer coefficients may be due to the difficulty in determining the boundary layer transitional region. Lack of close adherence to the assumptions of the experimental model may also contribute to the uncertainty in experimental heat transfer coefficients. Other causes may also include the circumferential separation between the gas temperature and the wall temperature measurements which should be made as close together as possible. Verification of these as sources of error should be the focus of additional experimentation with this technique. Uncertainty analysis, however, has shown that most of the analytical results and the steady state measurements are bracketed by experimental error bands on the transient data. Measuring heat transfer coefficients by a transient technique shows great potential for hostile environments such as jet engine hot sections. Particular attention, however, must be given to setting up the experiment within the assumptions of the experimental model.

TABLE 1. - STATOR VANE GEOMETRY

Mean diameter, cm	46.99
Vane height, cm	3.81
Axial chord, cm	3.81
Axial solidity	0.929
Aspect ratio	1.000
Number of vanes	36
Leading edge radius, cm	0.508
Trail 1g edge radius, cm	0.089

TABLE 2. - THIN FILM THERMOCOUPLE AND HEAT FLUX GAGE LOCATION

Pressure Surface			Suction Surface		
Sensor	x/L	Type	Sensor	x/L	Type
TTF34	0.170	Thin Film T/C	TTF25	0.140	Thin Film T/C
TTF10	.262	Thin Film T/C	TTF19	.424	↓
P3	.314	Heat Flux Gage	TTF20	.580	
TTF22	.354	Thin Film T/C	TTF28	.820	
TTF35	.354	Thin Film T/C			
TTF23	.540	Thin Film T/C			
P4	.587	Heat Flux Gage			
TTF24	.722	Thin Film T/C			
TTF36	.816	Thin Film T/C			

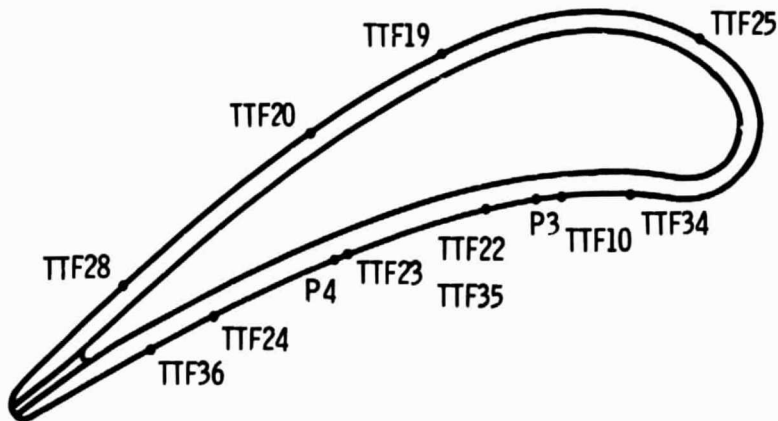


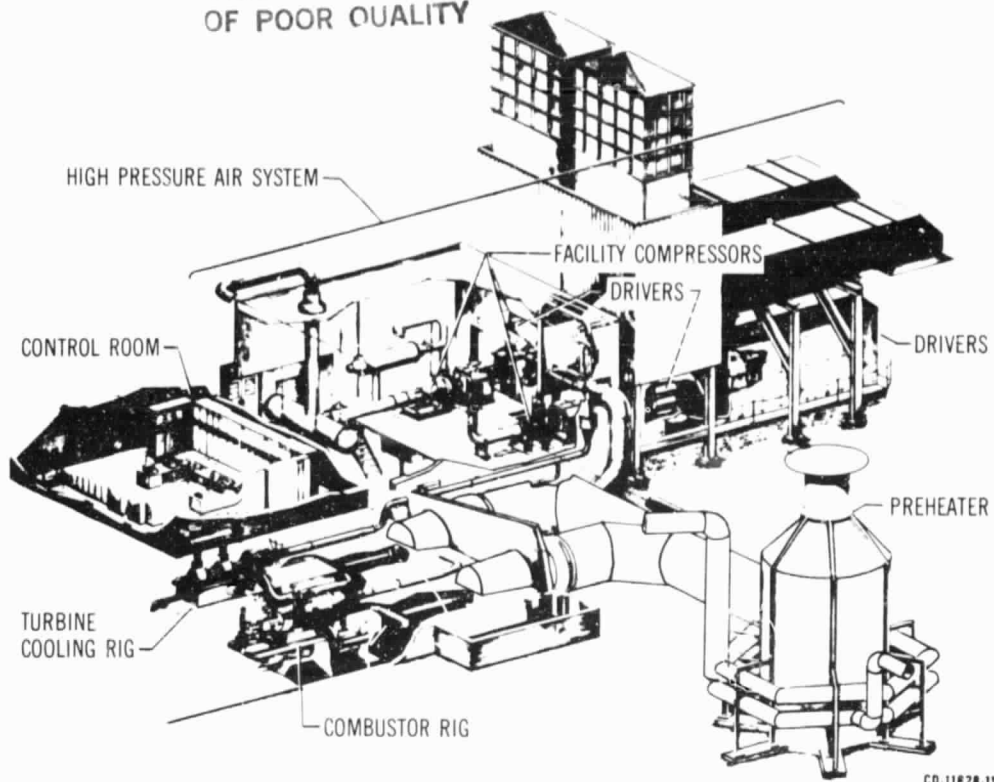
TABLE 3. - HSF CASCADE RESEARCH CONDITIONS

Case	Combustor Exit, Station 4		Coolant Temperature, K	Stator Exit, Station 5		Mode of operation	Frequency, Hz
	Temperature, K	Pressure, atm		Velocity ratio	Velocity ratio		
1a 1b	1280 1180	4.2 4.2	320	0.78	0.55x10 ⁶	10-atm	0.005, 0.0067, 0.01, 0.02, 0.05, 0.1, 0.2, 0.5
2a 2b	1290 1190	9.0 9.0			1.20x10 ⁶	10-atm	
3a 3b	1270 1180	9.0 9.0			1.20x10 ⁶	20-atm	0.005, 0.0067, 0.01, 0.02, 0.05, 0.1
4a 4b	1240 1150	12.9 12.9			1.90x10 ⁶	20-atm	

TABLE 4. - UNCERTAINTY ESTIMATES FOR THE GAS AND WALL TEMPERATURE MEASUREMENTS

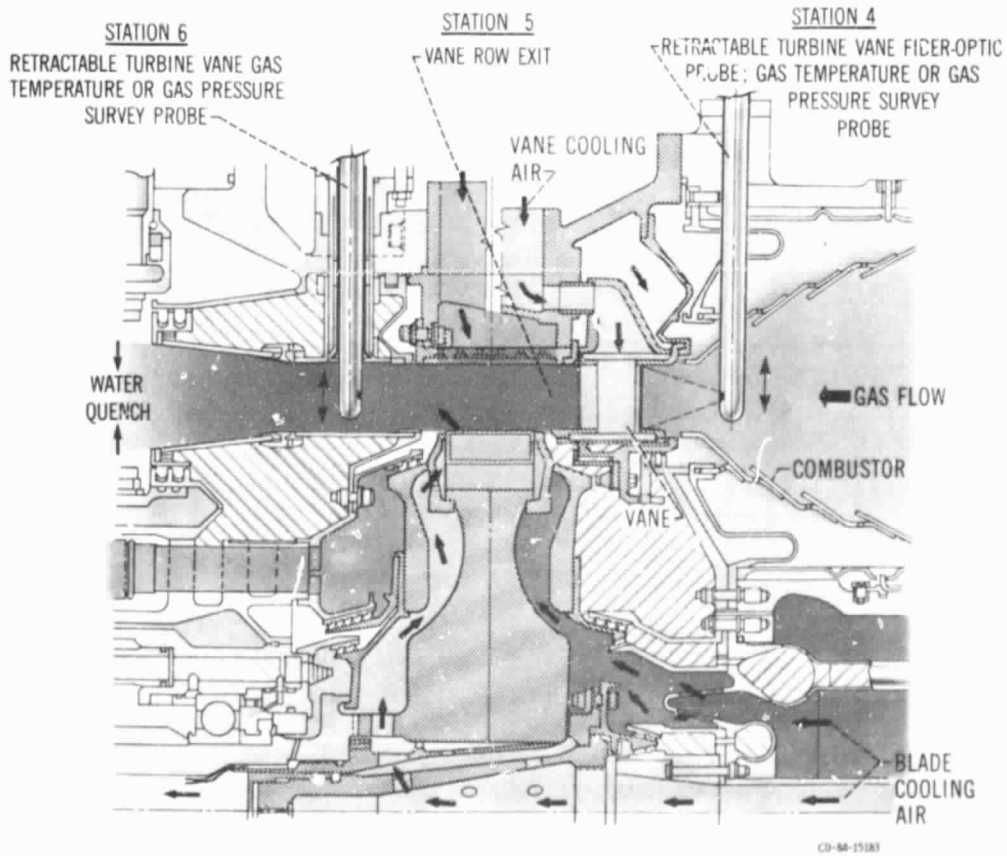
Instrument	Temperature, K	Uncertainty										Total rms, K	Percent	
		Sensor mat'l, K	Lead wire, K	Instru., K	Amplifier zero drift, K	Tape Recorder, K	Software Conversion, K	Recovery Correction, K	Radiation Correction, K	Conduction Correction, K				
Thin film thermocouple (wall temp)	810	+8.3	+1.4	+0.6	+1.1	+2.5	+1.1	-----	-----	-----	-----	-----	+8.9	1.6
Wall-element thermocouple (gas temp)	1255	+6.3	+0.5	+1.0	+0.5	+6.0	+1.0	+6.0	+7.5	+30	+32.7	3.3		

ORIGINAL PAGE IS
OF POOR QUALITY



CD-11828-11

(a) Perspective view



CD-84-15183

(b) Schematic of the combustor and the cascade vane row.

Figure 1. - Hot section test facility.

ORIGINAL PAGE IS
OF POOR QUALITY

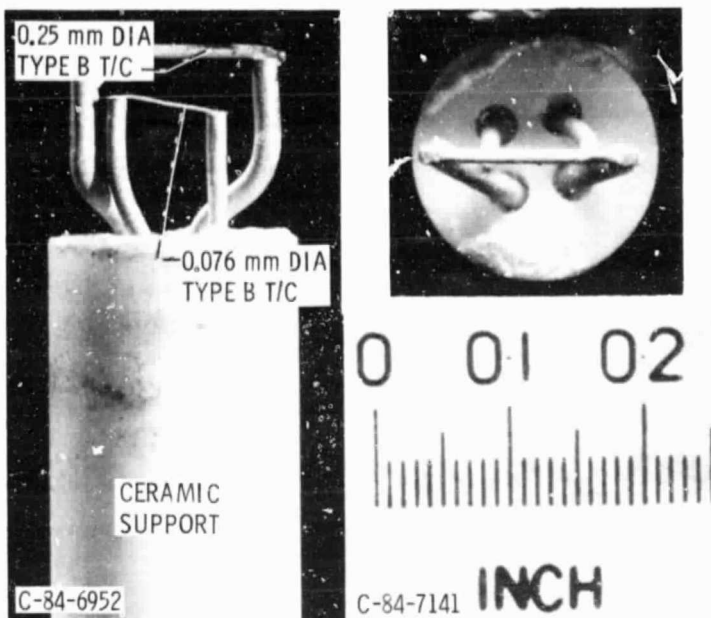


Figure 2. - Dual-element gas temperature probe.

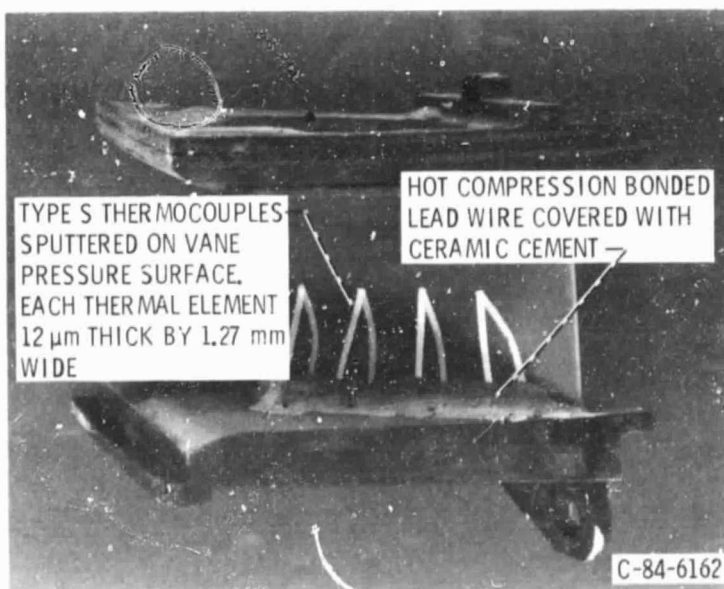


Figure 3. - Typical thin film thermocouple installation on an airfoil pressure surface. Lead wires have not been attached.

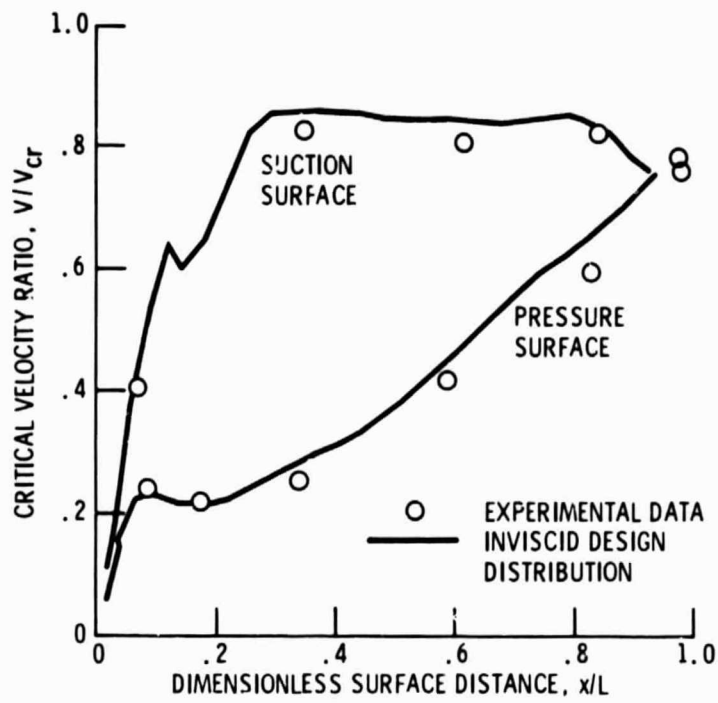


Figure 4. - Critical velocity ratio design conditions for the stator airfoil tested.

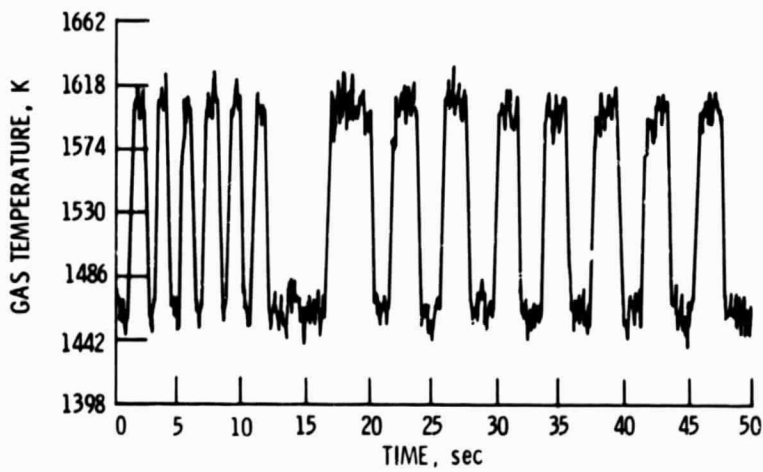
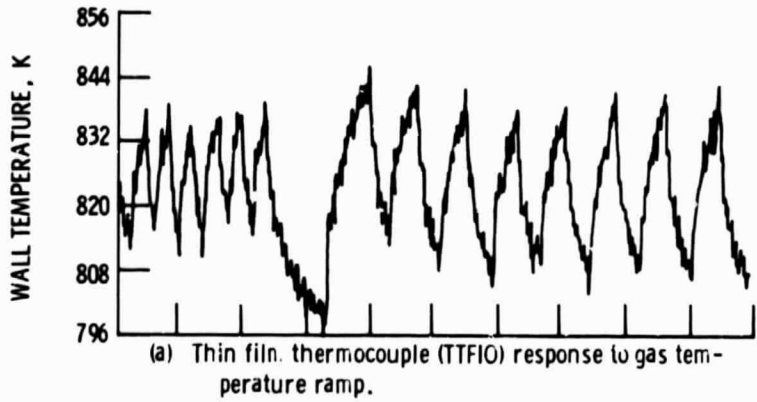


Figure 5. - Typical time histories of gas and wall temperatures during 2 and 4 second ramp cycles. Reynolds number = 1.2×10^6 .

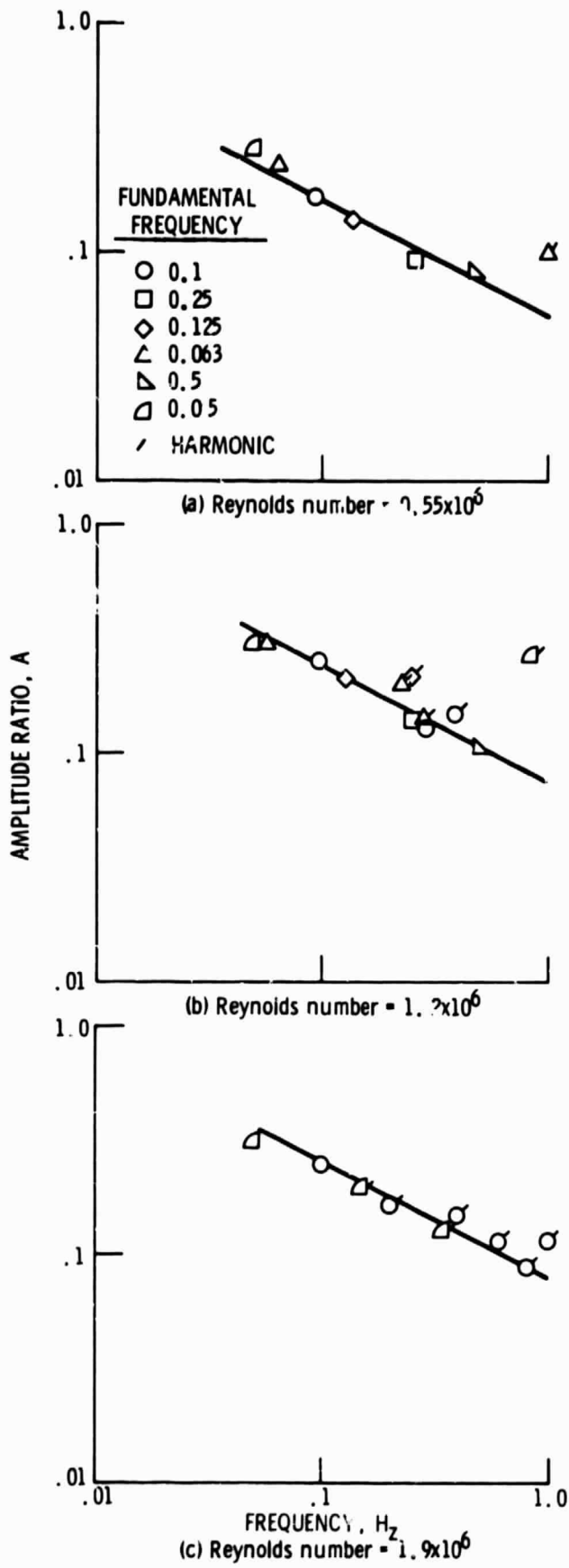


Figure 6. - Amplitude ratio of fourier components as a function of frequency for thin film thermocouple TTF10 located on the airfoil pressure surface.

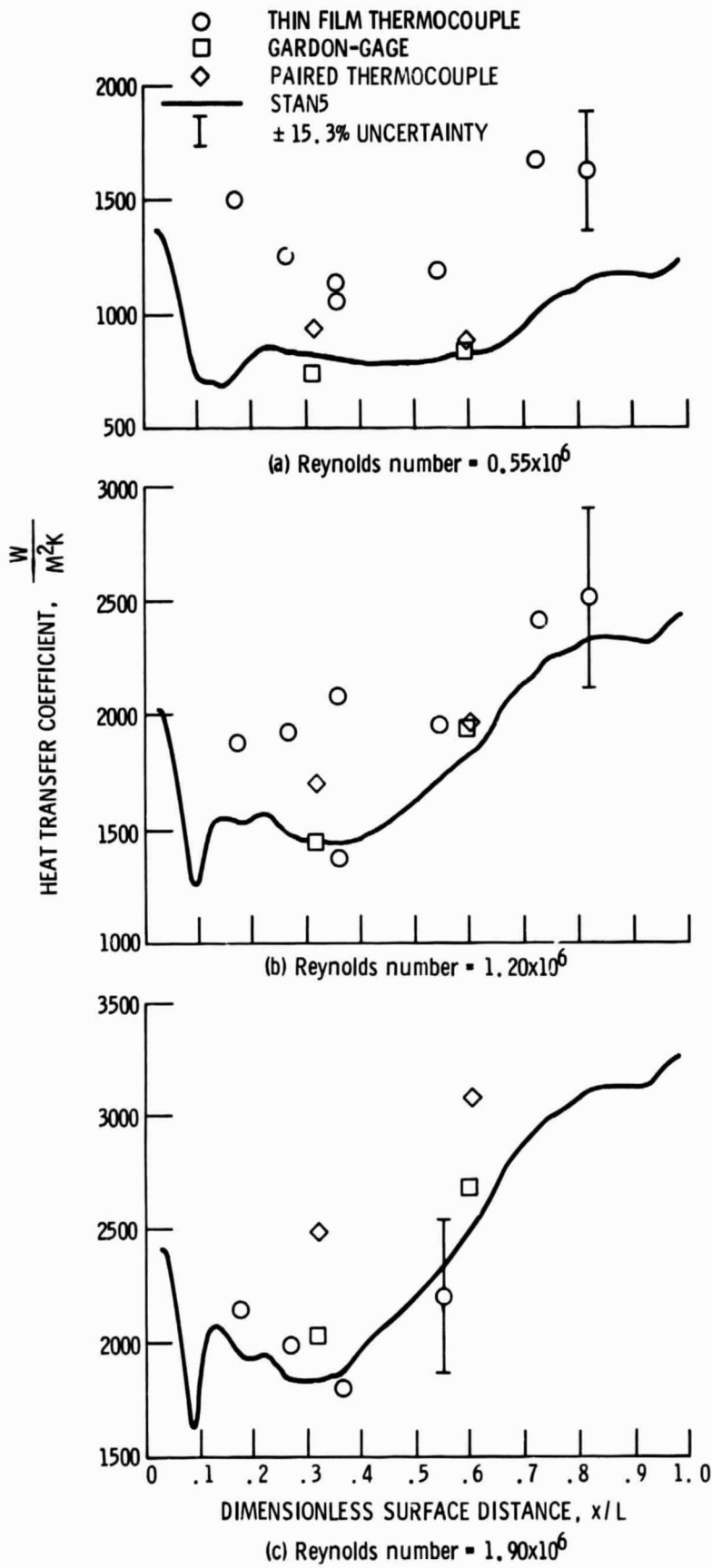


Figure 1. - Experimental heat transfer coefficient on the airfoil pressure surface are compared with STAN5.

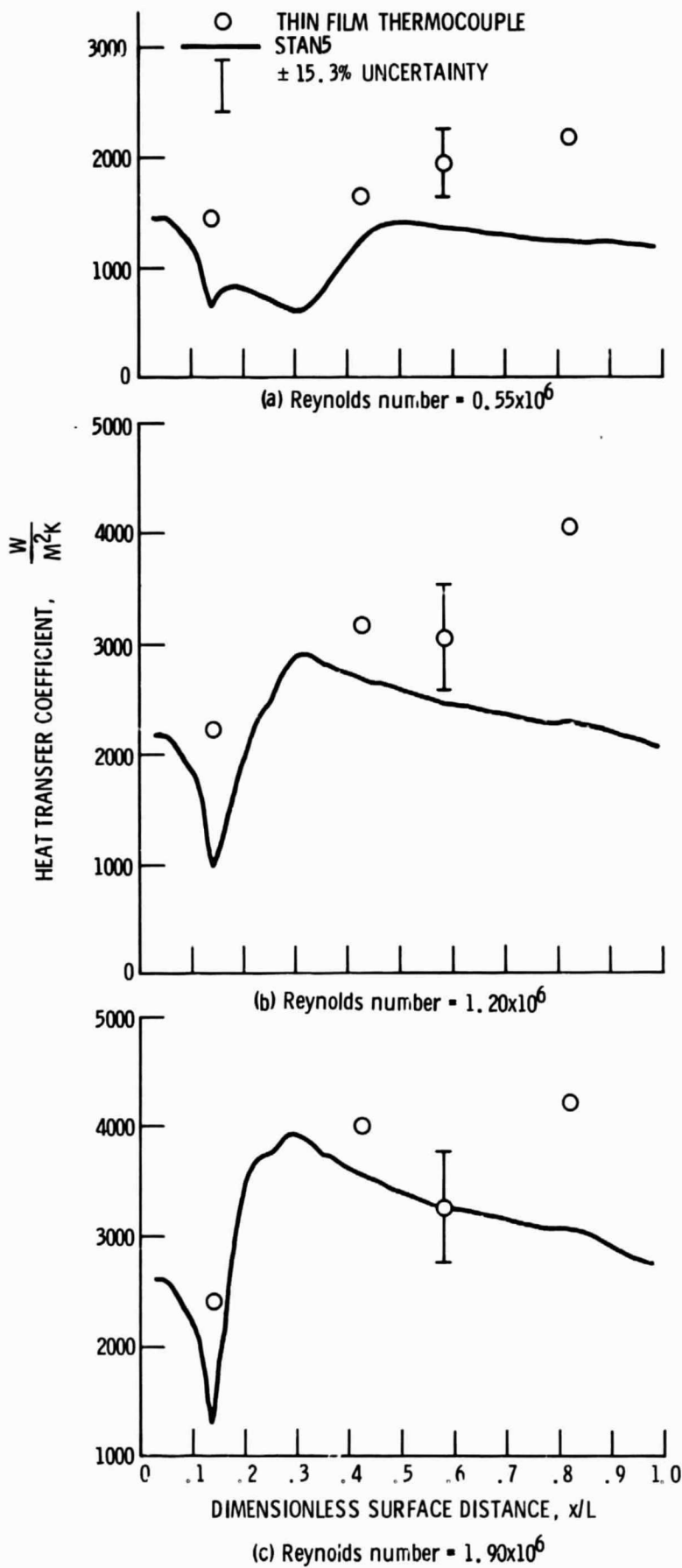


Figure 8. - Experimental heat transfer coefficients on the airfoil suction surface are compared with STAN 5.

1. Report No. NASA TM-87005		2. Government Accession No.		3. Recipient's Catalog No.	
4. Title and Subtitle Transient Technique for Measuring Heat Transfer Coefficients on Stator Airfoils in a Jet Engine Environment				5. Report Date	
				6. Performing Organization Code 505-31-04	
7. Author(s) Herbert J. Gladden and Margaret P. Proctor				8. Performing Organization Report No. E-2501	
				10. Work Unit No.	
9. Performing Organization Name and Address National Aeronautics and Space Administration Lewis Research Center Cleveland, Ohio 44135				11. Contract or Grant No.	
				13. Type of Report and Period Covered Technical Memorandum	
12. Sponsoring Agency Name and Address National Aeronautics and Space Administration Washington, D.C. 20546				14. Sponsoring Agency Code	
15. Supplementary Notes Prepared for the Twenty-first Joint Propulsion Conference cosponsored by the AIAA, SAE, and ASME, Monterey, California, July 8-10, 1985.					
16. Abstract A transient technique was used herein to measure heat transfer coefficients on stator airfoils in a high-temperature annular cascade at "real engine" conditions. The transient response of thin film thermocouples on the airfoil surface to step changes in the gas stream temperature was used to determine these coefficients. In addition, gardon gages and paired thermocouples were also utilized to measure heat flux on the airfoil pressure surface at steady state conditions. The tests were conducted at exit gas stream Reynolds numbers of one-half to 1.9 million based on true chord. The results from the transient technique show good comparison with the steady-state results in both trend and magnitude. In addition, comparison is made with the STAN5 boundary layer code and shows good comparison with the trends. However, the magnitude of the experimental data is consistently higher than the analysis.					
17. Key Words (Suggested by Author(s)) Heat transfer Coefficients Turbine cooling			18. Distribution Statement Unclassified - unlimited STAR Category 35		
19. Security Classif. (of this report) Unclassified		20. Security Classif. (of this page) Unclassified		21. No. of pages	22. Price*